Accepted Manuscript

Dalton Transactions

An international journal of inorganic chemistry

rsc.li/dalton

Volume 46
Number 10
14 March 2017
Pages 3073-3412

ISSN 0306-0012

ROYAL SOCIETY OF CHEMISTRY

COMMUNICATION
Douglas W. Stephan et al
N-heterocyclic carbene stabilized parent sulfenyl, selenenyl, and tellurenyl cations (XH+, X = S, Se, Te)

This is an Accepted Manuscript, which has been through the Royal Society of Chemistry peer review process and has been accepted for publication.

Accepted Manuscripts are published online shortly after acceptance, before technical editing, formatting and proof reading. Using this free service, authors can make their results available to the community, in citable form, before we publish the edited article. We will replace this Accepted Manuscript with the edited and formatted Advance Article as soon as it is available.

You can find more information about Accepted Manuscripts in the Information for Authors.

ROYAL SOCIETY OF CHEMISTRY

rsc.li/dalton

Structural, kinetics and mechanistic studies of transfer hydrogenation of ketones

catalyzed by chiral (pyridyl)imine nickel(II) complexes

Robert T. Kumah, Nokwanda Tsaulwayo, Bheki A. Xulu, Stephen O. Ojwach*

School of Chemistry and physics, University of KwaZulu-Natal, Pietermaritzburg Campus, Private Bag X01 Scottsville, 3209, South Africa

ABSTRACT

The chiral synthons (*S*-)-1-phenyl-N-(pyridine-2-yl)ethylidine) ethanamine (**L1**), (*R*-)-1phenyl-N-(pyridine-2-yl)ethylidine) ethanamine (**L2**) (*S*)-1-phenyl-N-(pyridine-2-yl methylene) ethanamine (**L3**), and (*R*)-1-phenyl-N-(pyridine-2-yl methylene) ethanamine (**L4**) were synthesized in good yields. Treatments of **L1-L4** with $NiBr_2(DME)$ and $NiCl_2$ precursor afforded dinuclear complexes $[Ni_2(\mathbf{L1})_4\text{-}\mu\text{-}Br_2]NiBr_4$ (**Ni1**), $[Ni_2(\mathbf{L2})_4\text{-}\mu\text{-}Br_2]NiBr_4$ (**Ni2**), $[Ni_2(\mathbf{L3})_4\text{-}\mu Br_2]Br_2$ (**Ni3**), $[Ni_2(\mathbf{L4})_4\text{-}\mu\text{-}Br_2]NiBr_4$ (**Ni4**) and $[Ni(\mathbf{L4})_2Cl_2]$ (**Ni5**). The identities of the compounds were established using NMR, FT-IR and EPR spectroscopies, mass spectrometry, magnetic moments, elemental analysis and single crystal X-ray crystallography. The dinuclear dibromide nickel complexes dissociate into mononuclear species in the presence of strongly coordinating solvents. Compounds **Ni1**-**Ni5** displayed moderate catalytic activities in the asymmetric transfer hydrogenation (ATH) of ketones, but with low enantiomeric excess (*ee*%). Both mercury and substoichiometric poisoning tests pointed to homogeneous nature of the active with partial formation of catalytically active Ni(0) nanoparticles. Low resolution mass spectrometry analyses of the intermediates supported a dihydride mechanistic pathway for the transfer hydrogenation reactions.

*Corresponding author: E-mail: ojwach@ukzn.ac.za (S. O. Ojwach)

1. Introduction

Asymmetric catalysis is one of the emerging disciplines in the chemical industry due to the versatility and importance of chiral intermediates in the production of a wide range of fine chemicals such as pharmaceuticals, perfumes, pesticides among others.[1-2] A classic example is the asymmetric transfer of hydrogenation (ATH) of ketones to produce chiral alcohols, which form useful intermediates for the syntheses of a number of domestically and industrial relevant products.[1, 3-5] To date, a number of transition metal catalysts derived from chiral ruthenium(II), rhodium(III), iridium(II), and osmium(II) metal complexes have been found to show high catalytic activities and enantioselectivities in asymmetric transfer hydrogenation of ketones.[6-12] Despite the efficiency of these catalytic systems in these reactions, their industrial application have been limited by their high costs and instability under normal conditions.[13-14]

This has led to the design and development of alternative catalysts which are less expensive but can parallel the catalytic activities of the well-established ruthenium(II) and iridium(II) analogues. On this trajectory, nickel(II) complexes have emerged as good candidates due to their relative cheaper costs and stability.[15-16] It is thus not surprising that in recent years, a number of nickel(II) catalysts containing nitrogen-donor ligands have been reported as catalysts[8] in the asymmetric transfer hydrogenation of ketones [17-18] The results have not been disappointing as high catalytic activities with excellent enantioselectivities have been reported in some cases. A notable example is the work of Gao and co-workers, which demonstrated that $Ni(PPh_3)_2Cl_2$ in combination with P^N^O-type ligands could catalyse ATH of simple ketones achieving 10-84 *ee*%.[19] We recently investigated the application of some (pyrazolylmethyl)pyridine nickel(II) complexes as catalysts in the transfer hydrogenation of ketones with some promising results.[20-21] Herein, we report the syntheses of chiral

(pyridyl)imine complexes and their application as ATH catalysts for a range of selected

aromatic ketones. Structural elucidation of the complexes has been extensively performed

using a combination of techniques such as mass spectrometry, electron paramagnetic

resonance, single crystal X-ray crystallography and elemental analyses. Detailed studies on

the true identity of the active species using substoichiometric and mercury poisoning tests and

investigation of the mechanistic pathways of ATH reactions have also been carried out and

are herein discussed.

2. Results and discussion

2.1. Synthesis and characterization Ni(II) complexes Ni1-Ni5

The reactions of synthons **L1-L4** with $NiBr_2(DME)$ and $NiCl_2$ in CH_2Cl_2 afforded the

corresponding complexes **Ni1-Ni5** as green solids (**Scheme 1**) in moderate yields (50-70%).

All the complexes were characterized by IR spectroscopy, mass spectrometry, magnetic

moment measurements, elemental analyses and single crystal X-ray analyses in some cases.

Comparison of FT-IR signal shifts of the ligands in **L1-L4** to their corresponding Ni(II)

complexes **Ni1-Ni5** allowed us to establish the successful formation of the complexes. For

instance, $(v_{C=N})_{imine}$ signals were observed at 1618 cm^{-1} for **L3** and 1637cm^{-1} for the

corresponding complex **Ni3** respectively (**Figs. S18 and S21**). The ESI-MS spectral data

were also used to establish the identity of the complexes **Ni1- Ni5 (Figs. S11-S15)**. In general,

ESI MS (low resolution) data of complexes **Ni1-Ni4** showed m/z signals corresponding to the

cationic mononuclear units, containing two ligand units. The absence of molecular mass peaks

corresponding to the dinuclear complexes hint to their instability, hence ease of dissociation

to form the mononuclear compounds (*vide infra*). For instance**,** the positive and negative

mode mass spectrum of complex **Ni4** showed signals at m/z = 559 amu and m/z = 373 amu,

corresponding to the fragment (M$^+$-Br$^-$) of the mononuclear species and the counter ion

[NiBr$_4$]$^{2-}$ respectively (**Fig. S21**). In all cases, the experimental and simulated isotopic mass

distributions showed correlations (**Figs. S18-S22**).
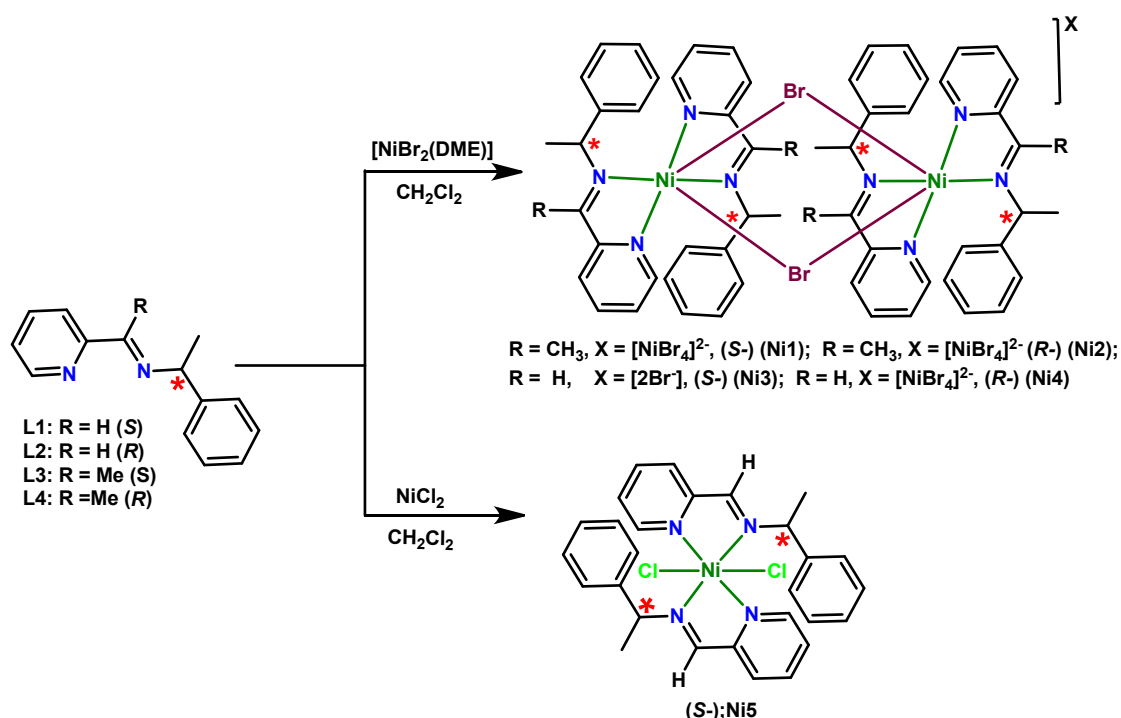
Scheme 1. Synthesis of chiral (pyridyl)imine Ni(II) complexes **Ni1-Ni5.**

The effective magnetic moments of complexes **Ni1-Ni5** were recorded in the range 3.52

BM - 3.97 BM and were generally higher than the expected spin-only magnetic moment of 2.83

BM for a nickel(II) ion.[22] This large variation could be attributed to the spin-orbital magnetic

moment contribution from the (pyridyl)imine and halide ligands.[23] However, all the values

were comparable, signifying similar ligand-field splitting of **L1-L4**. Elemental analyses data of

complexes **Ni1-Ni5** were in good agreement with two ligand units per metal atom and

established the purity of the bulk materials.

2.2. Molecular structure of compound Ni3 and Ni 4.

Single crystals suitable for X-ray crystallography analyses of complexes **Ni3a** (a monomeric form of **Ni3**) and **Ni4** were grown by slow evaporation of the CH_2Cl_2/hexane solutions at room temperature, while crystals of compound **Ni5** were obtained by slow diffusion of diethyl ether into a solution of **Ni5** in acetonitrile. **Table 1** shows the data collection and structural refinement parameters for complexes **Ni3a**, **Ni4 and Ni5**, while **Figs. 1-3** show the respective molecular structures and bond parameters. The solid state of complex **Ni4** is dinuclear containing two bidentate ligand units on each nickel atom, two bridging bromide ligands and a $[NiBr_4]^{2-}$ counter anion, in good agreement with the mass spectral and elemental analyses data (**Scheme 2**). On the other hand, the molecular structure of **Ni3a** (derivative of **Ni3**), is cationic, containing two ligand **L3** units per nickel atom (**Fig. 1**) and two coordinated water molecules. It is therefore evident that in the presence of strongly coordinating solvents such as H_2O, the dinuclear **Ni3** complex dissociates *via* nucleophilic substitution of the bridging bromides to form the mononuclear species (**Ni3a**) as shown in **Scheme 3**. The transformation is not unique and has been reported by Schlemper[24] and may be useful in generation of the activation species (creation of vacant coordination sites). Interestingly, the mononuclear dichloride complex **Ni5**, is neutral and contains two ligand (**L3**) units and two chloride ligands in the coordination sphere. The monomeric nature of **Ni5** thus indicate, unfavourable bridging by the chloride ligand, while the lack of substitution of the chlorides by the water molecules can be attributed to the poor nucleophilic displacement of the chloride ligands in comparison to the bromide ligand.[25]
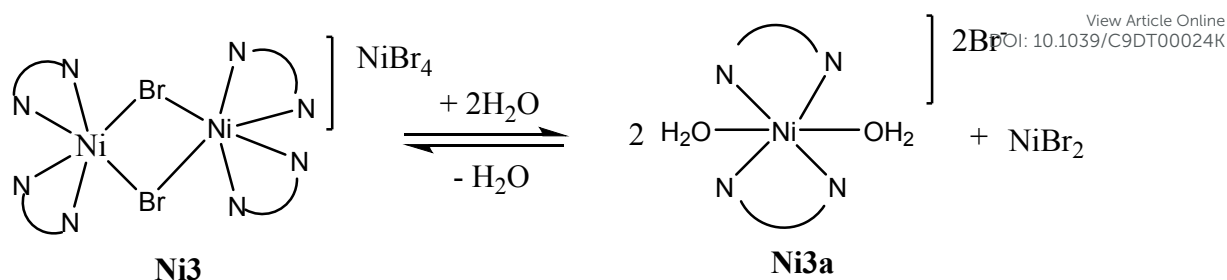
Scheme 3. Transformation of the dinuclear complex **Ni3** to the mononuclear species **Ni3a** in the presence of H_2O molecules via nucleophilic attack.

The average Ni-O, Ni-Br and Ni-Cl bond lengths of 2.068 Å, 2.595 Å and 2.417 Å for **Ni3a**, **Ni4** and **Ni5** are within the bond distances of 2.07±0.12 Å, 2.58 ± 0.08 Å and 2.42 ±0.06 Å respectively reported in 98-172 structures when subjected to online check CID routine data.[26-27] Similarly, the average Ni-N_{imine} bond lengths for **Ni3a**, **Ni4** and **Ni5** of 2.089 Å 2.079 Å, and 2.147 Å respectively, agree well with the average Ni-N_{imine} bond length of 2.123 Å reported in literature.[27] Furthermore, the Ni-N_{py} bond lengths of **Ni3a, Ni4** and **Ni5** of 2.06 Å, 2.088 Å and 2.033Å respectively are within the maximum range of 2.065 Å reported in literature.[27] The slight differences in for example, the averaged Ni-N_{imine} bond distances for **Ni3a**, **Ni4** and **Ni5** of 2.094(4) Å, 2.079 Å, and 2.150 (14) Å respectively may be attributed to the varied *trans* influence of the H_2O, bromide and chloride ligands. Interestingly, the bond distances of the Ni(1)-Nimine in the structure of **Ni3a** are quite different,despite having the same H_2O ligand in the trans-position. The reason for this variation is not clear, though steric factors may be implicated.

Table 1: Crystal data and structure refinement parameters for complexes **Ni3a** and **Ni4**.

Parameter	Ni 3a	Ni 4	Ni5
Empirical formula	2($C_{28}H_{32}N_4NiO_2$),4(Br),H_2O	C56 H56 Br6 N8 Ni3	C28H28N4NiCl2
Formula weight	1368.22	1496.67	550.15
Temperature(K)	100	100(2)	100
Wavelength (Å)	0.71073	0.71073 Å	0.71073
Crystal system	Monoclinic	Orthorhombic	Monoclinic
Space group	P 21	P 21 21 21	P1 21 1
a(Å)	9.4714(5)	13.3668(9)	8.4920(7)
b(Å)	15.4585(7)	24.1182(16)	18.0236(14)
c(Å)	19.8142(10)	24.2402(16)	8.5613(7)
$\square$(°)	90	90	90
β(°)	91.8 (3)	90	99.564
γ (°)	90	90	90
Volume	2899.6(2)	7814.6(9)	1292.15(18)
Z	2	4	2
Dcalcd (mg/m3)	1.567	1.272	1.414
Absorption coefficient (mm^{-1})	3.459	3.816	3.448
F(000)	1388.0	2968	572
Number reflections	0.0254(10895)	56652	6204
Goodness-of-fit on F2	1.001	1.060	1.002
R indices (all data)	R1=0.0254, wR2=0.0555	R1=0.0394,wR2= 0.0707	R1=0.0173, wR2=0.044
Largest diff. peak and hole (e Å^{-3})	0.660 and -0.265	1.403 and -0.773	0.1433 and - 0.254

The bond angles of 79.86(14)°, 90.17(13)° and 91.50(13)° for N(1)-Ni(1)-N(2), N(1)-

Ni(1)-O(1), O(1)-Ni-O(1) respectively for **Ni3a** deviate slightly from the expected 90° and

thus reveal a distorted octahedral geometry. Similar distortion is observed in complex **Ni5,** with most bond angles recorded within the range 78°-98°. In general, the presence of two ligand units around each nickel(II) atom in complex **Ni4** is not common for dinuclear nickel(II) complexes and may largely be attributed to the less steric demands of ligands **L1-L4**.
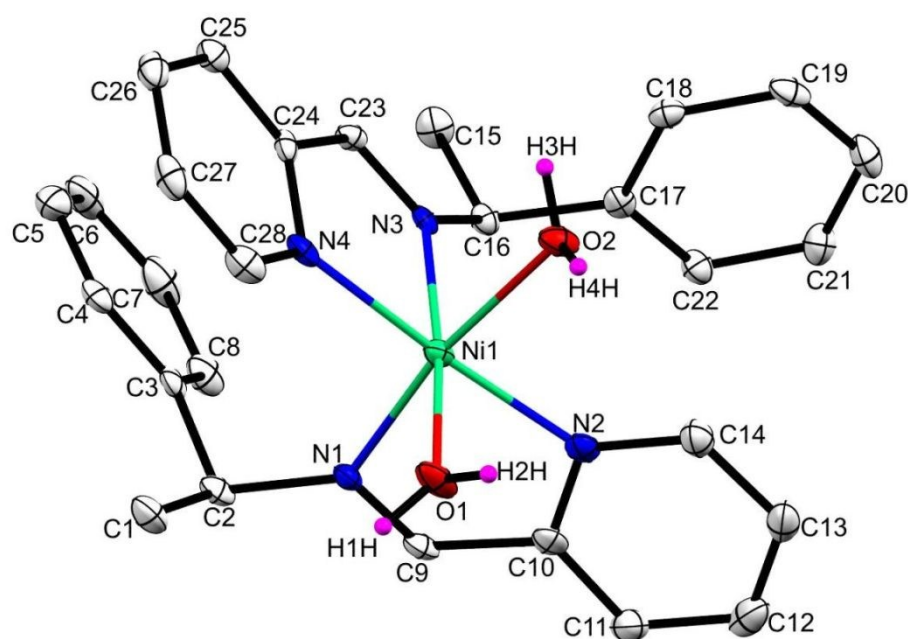
Fig. 1: Symmetric unit of compound **Ni3a** with thermal ellipsoids drawn at 50% probability level. H, Br and H_2O atoms were omitted for clarity. Bond lengths (Å); Ni(1)-N(1), 2.121(4); Ni(1)-N(2), 2.064; Ni(1)-N(3), 2.067(4); Ni(1)-N(4), 2.073(4); Ni(1)-O(1), 2.055(4); Ni(1)-O(2), 2.092(3); Ni(1)-N(4), 2.055(4); Bond angle (°); N(2)Ni(1)-N(3), 99.4 (14); N(2)-Ni(1)-O(2), 89.9(14); N(3)-Ni(1)-O(2), 88.4(13); N(4)-Ni(1)-O(2), 86.0(13); N(3)-Ni(1)-N(4), 80.3(14); N(2)-Ni(1)-N(4), 175.9(14).

Dalton Transactions Accepted Manuscript
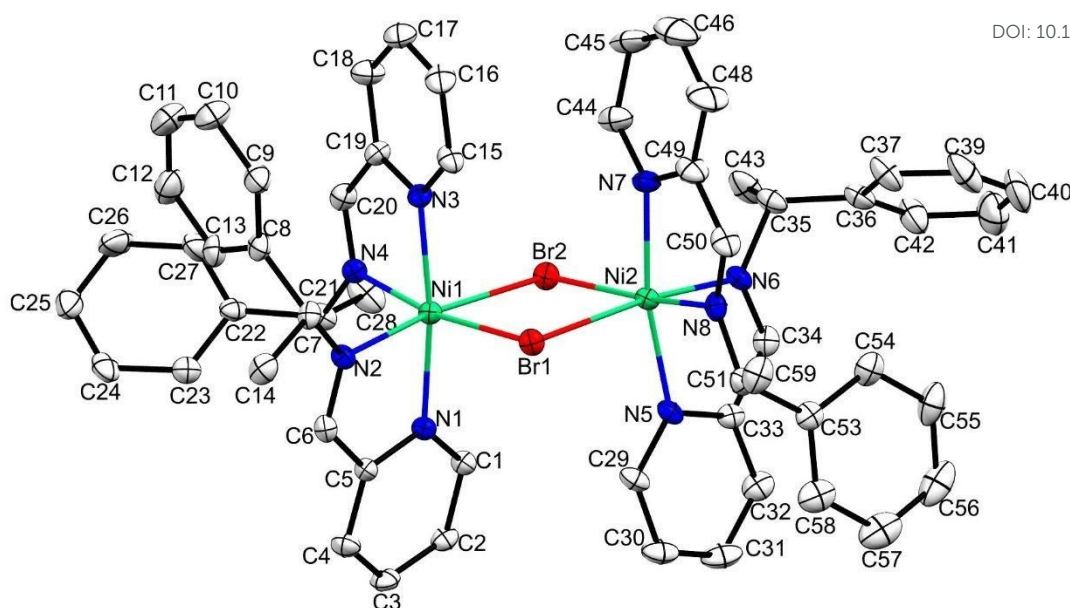
Fig. 2. Thermal ellipsoids (40% probability) plot of complex **Ni4.** H atoms and [NiBr$_4$]$^{2-}$ were omitted for clarity. Bond lengths (Å); Ni(1)–N(1), 2.089(4); Ni(1)–N(2), 2.079(4); Ni(1)–N(3), 2.084(4); Ni(1)–N(4), 2.081(4); Ni(1)–Br(1), 2.568(7); Br(3)–Ni(2), 2.546(7); Br(6)–Ni(3), 2.379(9). Bond angle (°): Ni(1)–Br(1)-Ni(2), 91.4(2); Ni(2)-Br(2)-Ni(1), 92.4(2); N(1)-Ni(1)N(2), 79.9(14; N(1)-Ni(1)-Br(1), 94.9(10), N(3)-Ni(2)-Br(2), 90.2(10); N(5)-Ni(2)-N(7), 79.5(17).

Dalton Transactions Accepted Manuscript
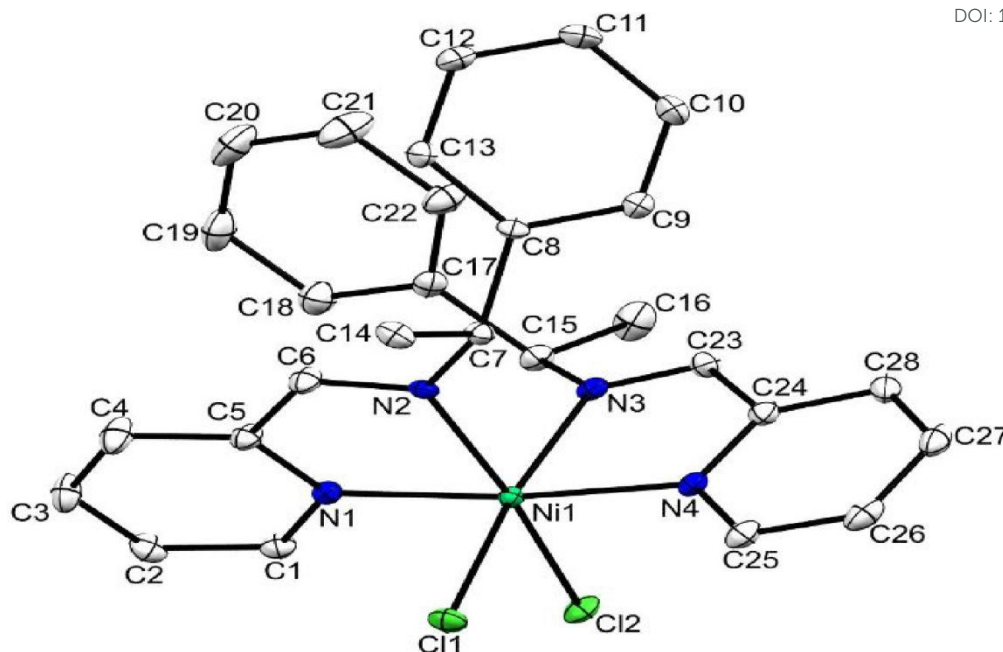
Fig. 3. Molecular structure of complex **Ni5** draw with thermal ellipsoids (50% probability). Hydrogen atoms were omitted for clarity. Bond lengths (Å); Ni(1)–N(1), 2.033(15); Ni(1)– N(2), 2.147 (14); Ni(1)–N(3), 2.153 (13); Ni(1)–N(4), 2.0361(16); Ni(1)–Cl(1), 2.396(5); Cl(2)–Ni(1), 2.438 (5). Bond angle (°): N(1)–Ni(1)-Cl(1), 90.41(4); N(1)-Ni(1)-N(3), 98.05(6); N(1)-Ni(1)-N(2), 78.67(6); N(1)-Ni(1)-Cl(2), 169.42(42), N(4)-Ni(1)-N(3), 78.76(10); N(4)-Ni(1)-N(2), 95.40(6).

2.3. Electron paramagnetic resonance (EPR)

The X-band EPR spectra of nickel(II) complexes, **Ni3**, **Ni4** and **Ni5** were recorded at room temperature and 77 K. Both powder and frozen solutions of **Ni3, Ni4** and **Ni5** exhibited broad isotropic signals (**Fig. 4(a)** and **(b)**). The g_{iso} values measured for these complexes (2.20-2.32) are much higher than those expected for nickel(II) species and organic radicals of g ≈ 2.00.[28] However, the g_{iso} values in the range 2.20-2.32 are typical for paramagnetic nickel(II) centers.[29] Surprisingly, the ESR spectrum of **Ni4** in DMSO (a strong coordinating solvent) at room temperature is similar to that of ^{i}PrOH (a weakly coordinating solvent) suggesting non-coordination (**Fig. 4(a)**). The use of CH_3CN, a moderately strong coordinating solvent only

resulted in broader line widths and no significant change in the g value recorded compared to weakly coordinating iPrOH solvent (**Fig. 4**). The simulated epr spectra in the solid state of complexes **Ni4** and **Ni5** compare well with the experimental spectra (**Fig. 4(c)** and **(d)).**
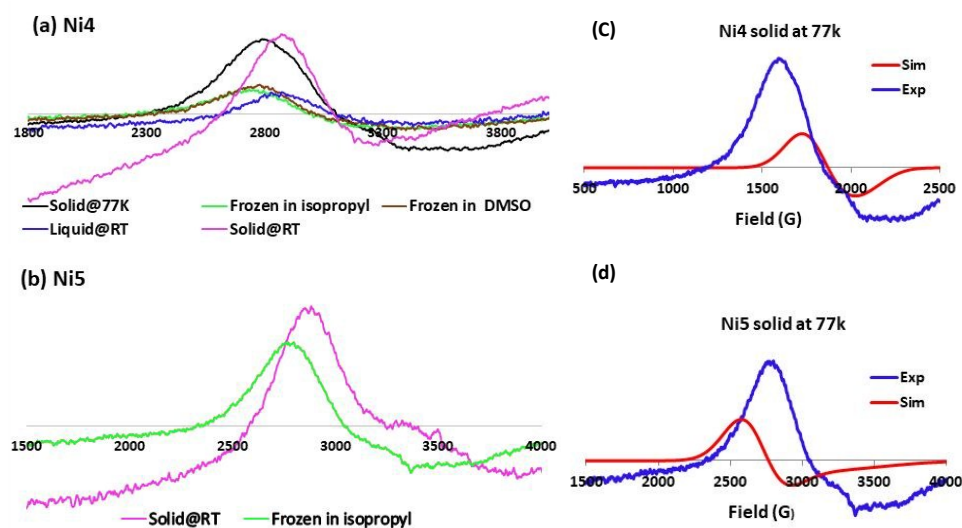
Fig 4. EPR spectra data of (a) **Ni4**; solid at room temperature (g=2.24), frozen in iPrOH (g = 2.21), Frozen in DMSO (g=2.28), frozen at 77 (g=2.25) and (b) **Ni5**; solid at room temperature (g=2.24), Frozen in iPrOH (g =2.22) (g =2.20). Simulated and experimental epr spectra of complexes **Ni4 (c)** and **Ni5** (**d**) respectively.

2.4. Asymmetric transfer hydrogenation of ketones.

*2.4.1. Screening of Ni(II) complexes **Ni1-Ni5** in asymmetric transfer hydrogenation of acetophenone.*

The Ni(II) complexes **Ni1-Ni5** were evaluated in catalytic transfer hydrogenation of ketones using acetophenone, KOH and ^{i}PrOH as the model substrate, base and hydrogen donor respectively. Percentage conversions and enantiomeric excess of the substrate to the respective *R/S*-alcohols were determined by ^{1}H NMR spectroscopy (**Fig. S23**) and chiral GC analyses (**Fig. S24**). All the complexes showed modest conversions between 54% and 98% (TOF = 7.50 and 13.61 h^{-1}) within 24 h (**Fig. S25** and **S26**) though with very low *ee* of between11% to 16% (**Table 2**). Based on these findings, we thus carried out detailed investigations of the kinetics, insights into the mechanistic pathways, deactivation profiles and nature of the active species of these ATH reactions.

2.4.2 .Effects of complex/ ligand structure on ATH of acetophenone

To understand the effects of ligand/complex structure on the kinetics of the ATH of acetophenone catalyzed by complexes **Ni1**-**Ni5**, plots of In[Acetoph.]$_{o}$/[Acetoph.]$_{t}$ versus time (**Fig S26**) were used to deduce the initial rate constants, k_{ob} for each complex and the order of reaction with respect to acetophenone substrate. A *pseudo*-first order kinetics with respect to acetophenone substrate was deduced from the linear section of the plots (**Fig. S26** inset) as shown in equation 1.[30] The rate constants (k_{ob}) and the corresponding TOFs for complexes **Ni1-Ni5** are given in **Table 2** and the initial rate constants were in the order **Ni4>Ni3>Ni5>Ni1>Ni2**.

Dalton Transactions Accepted Manuscript

$$\text{Rate} = k_{ob}[\text{acetoph.}]^1 \dots\dots\dots\dots\dots\dots\dots\dots\dots \text{(Eq. 1)}$$

From the catalytic activity trends obtained with respect to the ligand architecture, complexes bearing methyl substituent on the imine carbon showed lower catalytic activities compared to the unsubstituted counterparts. For example, complex **Ni1** bearing a methyl substituent recorded a lower k_{ob} of 4.0 x $10^{-5} s^{-1}$ compared to the unsubstituted analogous complex **Ni3**, which achieved k_{ob} of 4.7 x $10^{-5} s^{-1}$ (**Table 2**, entries 1 and 3). While it is much easier to assign this trend to steric effects (CH_3 vs H), a closer examination of the structures reveals that this groups are remotely located away from the metal atoms hence unlikely to confer any significant steric control. Thus, we believe that the lower reactivity of complex **Ni1**, bearing the methyl substituents may be due to reduced electophilicity of the Ni(II) atom (since CH_3 is more electron donating than H group). This has the net effect of limiting substrate coordination to the active metal centre. These results are in agreement with literature findings of Chirik *et al*,[31] where diimine Fe(II) complexes bearing methyl substituent at the imine carbon in the ligand backbone showed lower catalytic than unsubstituted diimine Fe(II) complexes in asymmetric hydrosilylation of acetophenone.

Table 2. Kinetic data of catalytic asymmetric transfer hydrogenation of acetophenone catalyzed by complexes **Ni1-Ni5**

Entry	Catalyst	Conversion [%][b]	Initial rate constant k_{ob} x 10^{-5}/s-1	R_2	TOF/h^{-1}	Enantiomeric excess (*ee* %)
1	**Ni1**	54	4.00±0.04	0.98	7.86	11(*S*-)
2	**Ni2**	72	5.52±0.06	0.98	10.00	16(*R*-)
3	**Ni3**	84	4.73±0.03	0.98	11.66	6(*S*-)
4	**Ni4**	98	7.55±0.11	0.99	13.60	11(*R*-)
5	**Ni5**	88	7.02±0.08	0.97	11.79	14 (*R*-)

[a] Conditions: acetophenone, 2.00 mmol; catalyst; 0.057 mmol (0.3 mmol%); base, (100 mmol%) KOH in 2-propanol (5.0 ml); time, 24 h, temperature, 82 °C. [b] Determined by ^{1}H NMR spectroscopy. [c] Turn over frequency (TOF) = (mmol of substrate)/(mmol of catalyst)/(h).

The stereochemistry of the complexes was also observed to influence the catalytic activities of the resultant catalysts. For example, complex **Ni4** (*R*-) showed high k_{ob} of 7.55 x 10^{-5}/s^{-1} compared to the corresponding complex **Ni3** (*S*-) of 4.73 x 10^{-5}/s^{-1} (**Table 2**, entries 34). Thus for the (*S*-) isomer (**Ni3**), the close proximity of the bulkier phenyl groups to the Ni atom is likely to hinder coordination of acetophenone substrate, accounting for the lower catalytic activity observed. This observation is consistent with those of Morris *et al* where (*R,R*)-*trans*-[Fe(CO)Me(CN)-CyP$_2$N$_2$][BF$_4$] catalysts were observed to show high catalytic activity than (*S,S*)-*trans*-[Fe(CO)Me(CN)-CyP$_2$N$_2$][BF$_4$] (*R,R*).[13] While the remote location of the chiral centre outside metal coordination may be implicated in the low ee% recorded for these catalysts, it is also possible that dissociation of the complexes into ligandless nickel(0) salts, may play a major role in their poor enantiaoselectiviy.

In comparison to the previously reported nickel-based catalysts in the transfer hydrogenation of ketones, these present catalysts display moderate catalysts. For example, the k_{ob} observed for the nickel complexes **Ni1**-**Ni4** of between 4.00 to 7.02 x 10^5 s^{-1} are slightly higher than the values of 2.5 to 5.0 x 10^5 S^{-1} reported for the (pyrazolylmethyl)pyridine nickel complexes.[20] In addition, the complexes **Ni1**-**N4** showed better catalytic activities compared to the template Ni(0) systems of Ni(COD)$_2$/dppe which gave conversions of 96% only after 48 h at elevated temperatures of 130 ^{0}C.[32] In terms of enantioselectivity, the complexes **Ni1**-**N4** (ee% < 11%) fared poorly compared to Ni(PPh$_3$)$_2$Cl$_2$/P^N^O- systems that could catalyse ATH of simple ketones to achieve 10-84 *ee*%.[19]

2.4.3. Optimization of reaction conditions on transfer hydrogenation

Upon establishing the catalytic efficacy of the nickel complexes **Ni1**-**Ni5** in the transfer hydrogenation of acetophenone, we then optimized the reaction conditions by investigating the effect of base and catalyst loading using the most active complex **Ni4**. Generally, an increase in catalyst loading was observed to result in diminished catalytic activities. For example, an

increase in catalyst loading from 0.30 mmol% to 1.14 mmol%, was followed by a drastic

decrease in TOF from 13.47 to 2.19 h^{-1} (**Table 3**, entries 1 and 4 and **Fig. S27**). Decrease in

catalytic activity with increase in catalyst loading may be associated with the aggregation of

the pre-catalysts[20, 33-34] which have the net effect of reducing the number of active species. This

agrees with the literature reports by Rupesh *et al* where an increase in catalyst/substrate ratio

from 1:400 to 1:1600 resulted in drop in catalytic activities from 90% to 46% within 3 h for

Ru(II) carbonyl benzoylhydrazone complex.[35] On the other hand, lower catalytic activities

observed at lower catalyst loadings of 0.14 mmol% pointed to possible insufficient amount of

the active species, thus rendering 0.30 mmol% as the optimum catalyst loading (**Fig. S27**). The

impact of the nature of the base on the ATH of acetophenone was also studied by using *t*BuOK**,**

KOH, NaOH, and Na$_2$CO$_3$ (**Table 3**, entries 5-8). The highest catalytic activity was observed

in *t*BuOK, while the lowest catalytic activity was recorded in Na$_2$CO$_3$. This is consistent with

the order of pK$_b$ values (base strength) and stability of the bases in good agreement with

literature findings.[36]

Table 3. Effect of catalyst loading and nature of base in ATH of acetophenone using
complex **Ni4**

Entry	Base	Catalyst loading/mmol %	Conversion[%]	TOF/h^{-1}
1	KOH	0.30	97	13.47
2	KOH	0.14	53	15.80
3	KOH	0.43	72	6.98
4	KOH	0.86	64	3.10
5	KOH	1.14	60	2.19
6	NaOH	0.30	96	13.33
7	^{t}BuOK	0.30	99	13.75
8	Na$_2$CO$_3$	0.30	66	9.16

[a]Conditions: acetophenone, 2.00 mmol; catalyst, 0.0057 mmol (0.30 mmol%); 100 mmol% of base in 2-propanol (5.0 mL), time, 24 h; temperature, 82 °C. [b]Determined by ^{1}H NMR spectroscopy; [c]Turn over frequency (TOF) = (mmol of substrate)/(mmol of catalyst)/time.
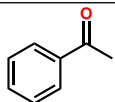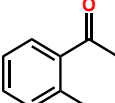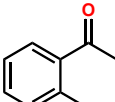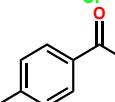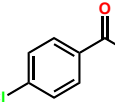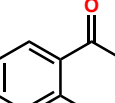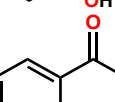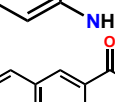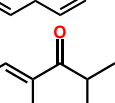
2.4.4. Variation of ketones substrates

Having established the optimum reactions conditions for the TH reactions, we turned our attention to the scope of ketone substrates that can be reduced by nickel complex **Ni4** (**Table 4**). In general, acetophenone derivatives bearing electron donating or withdrawing groups appeared to exhibit lower reactivities (**Tables 4**, entries 1-4). For example, 2-methylacetophenone and 2-chloroacetophenone displayed conversions of 87% and 91% compared to 98% respectively repo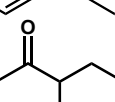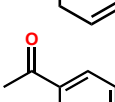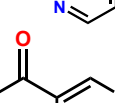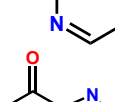rted for acetophenone (**Table 4**, entries 1-3). This trend contradicts previous literature findings for Ni-N^P^O and Fe(II) (NH)$_2$P$_2$ catalysts where higher reactivities (>95%) were observed for acetophenone derivatives bearing electron donating or withdrawing groups compared to acetophenone (81%).[19, 37-38] The observed trend could be attributed to steric effects, since the substituents are at the *ortho* position, which is close to the carbonyl centre. The argument is supported by the lower reactivities observed for the more sterically demanding 2-aminophenyl acetophenone and cyclohexyl acetophenone of 80% and 86% respectively (**Table 4**, entries 1, 5 and 6). Indeed, the less sterically hindered 1-

Dalton Transactions Accepted Manuscript

(naththalen-2-yl) ethan-1-one recorded relatively higher percentage conversion of 93 %

conversions (Table 4, entry 8). These results compare well with those reported by Ikariya *et al.*

using oxo-tethered Ru(II) complexes where sterically hindered benzophenone, gave lower

catalytic activities >59 % compared to conversions of >99% for the unsubstituted

benzophenones. We also studied *para*-substituted acetophenones using 4-methylacetophenone

and 4-chloroacetophenone substrates (Table 4, entries 4 and 5). Interestingly, lower reactivities

of 57% and 87% were recorded for 4-methylacetophenone and 4-chloroacetophenone

respectively, a phenomenon that can be largely attributed to electronic effects. Heterocyclic

aromatic ketones also exhibited lower conversions. For example, conversions of 56% and 49%

were recorded for the pyrazine and pyrrole derivatives respectively (**Table 4**, entries 1 vs 11-

13) in line with irreversible coordination of the heteroatoms to the metal center.[39] [14]

Interestingly, there was no significant drop in catalytic activity for the aliphatic 1-cylcohexyl

ethanone ketone (93%) (**Table 4**, entry 10).

Table 4. Effect of substrate scope variation on the TH reactions catalyzed by complex **Ni4**

Enter	Substrate	Conversion[%]	TOF/h^{-1}

1		98	13.68
2		87	12.08
3		91	12.63
4		57	7.97
5		87	12.08
6		92	12.77
7		86	11.94
8		93	12.91
9		80	11.10
10		63	8.74
11		89	12.35
12		56	7.77
13		49	6.80

[a] Conditions: acetophenone, 2.00 mmol; 0.0057 mmol (0.3 mmol%); base, ^{t}ButOK(100 mmol%) in 2-propanol (5.0 ml); time, 24 h, temperature, 82 °C. [b] Determined by ^{1}H NMR spectroscopy. [c] Turn over frequency (TOF) = (mmol of substrate)/(mmol of catalyst)/(h).

2.5 Determination of the nature of the active species

In modern catalytic practises, determination of the true nature of the active species is a ubiquitous exercise and regarded as a bare minimum. In distinguishing between homogeneous

and heterogeneous catalysts, a number of experiments such a catalyst poisoning tests and identification of nanoparticle formation are employed.[40-43] We thus employed sub-stoichiometric and mercury poisoning experiments to determine the true active intermediate.[44-46] Using 20% (mol. equivalent to **Ni4** complex) of tricyclohexyl phosphine (PCy$_3$), triphenylphosphine (PPh$_3$), and carbon disulfide (CS$_2$), we observed appreciable reduction in conversions of complex **Ni4** from 85% to about 65%, 60% and 45% respectively (**Fig. 5**). This diminished catalytic activity upon addition of 20% of the poisoning ligands provided points to a possible existence of catalytic active Ni(0) nanoparticles, i.e heterogeneity of the system. However, the significant percentage conversions retained in the presence of the poisons of 45% - 65% (representing about 50% to 75% of the original catalytic activity) is a strong indicator of largely homogeneous species.[41] Indeed, the observation of catalytic activities (conversions of 55%) even upon addition of 100% mol equivalent of PPh$_3$ (**Fig. S29**) corroborates this assertion.
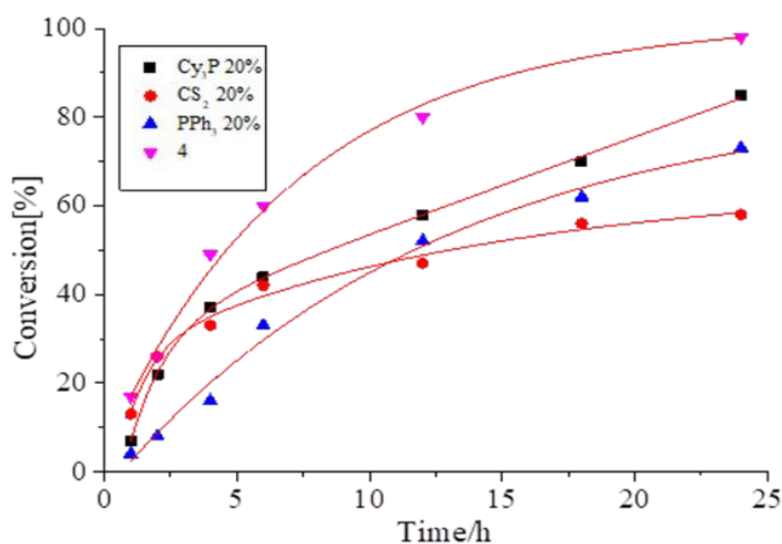
Fig. 5. Kinetics of the deactivation profiles of catalyst **Ni4** using 20% (mol equivalent to the **Ni4** catalyst) phosphine ligands PCy$_3$, PPh$_3$ and CS$_2$.

To gain further insight in the nature of the active species of complex **Ni4**, we carried out mercury poisoning tests using 3, 5 and 10 drops at the beginning of the reaction (after pre-generation of the active species) and at about 50% conversion (**Fig. 6** and **Fig. S29**). Both experiments were run for 24 h and compared to the control experiments without mercury (**Fig. 6**).[40, 47-49] Lower conversions of about 60% (initial addition) and 66% (50% addition) were observed in comparison to conversions of 98% reported in the absence of mercury. The partial reduction in catalytic activity of complex **Ni4** points to the presence of both homogeneous and Ni(0) nanoparticles as the active species, in good agreement with the sub-stoichiometric data.[41, 50] From the the poisoning data and smooth kinetics curves (Figs. **S25** and **S26**), we can conclude that active species are largely homogenous in nature but accompanied by the formation of catalytic active Ni(0) nanoparticles during the course of the reaction.[41]
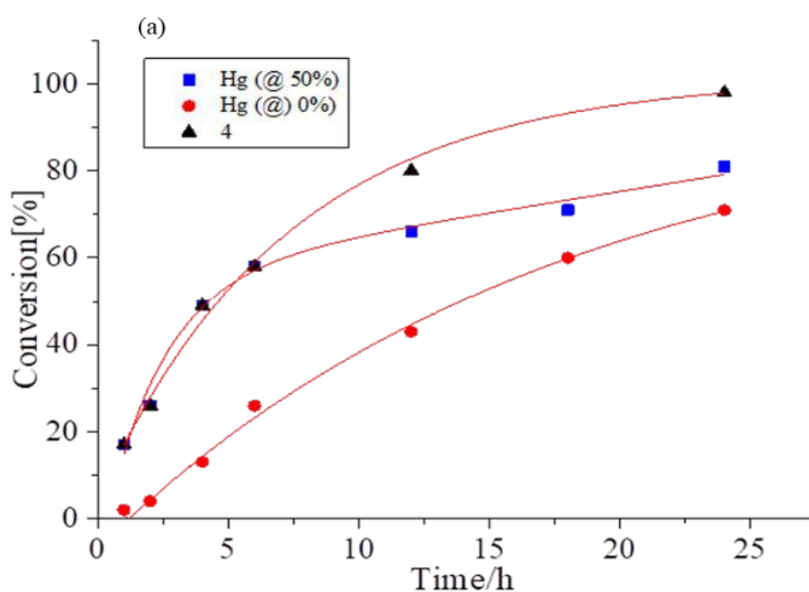
Fig. 6. Kinetic plots showing deactivation profiles of complex **Ni4** with excess mercury. The deactivation experiment was carried out using 5 drops of Hg at the beginning and at 50% percentage conversions and compared with the standard kinetic profiles.

2.6 Proposed mechanism of asymmetric transfer hydrogenation of ketones catalyzed by complex Ni4

Having established the homogeneity of the active species of complexes **Ni1–Ni5**, we therefore employed low resolution mass spectrometry to support the plausible mechanism for the ATH reactions of complex **Ni4** (**Fig. S28**) as given in **Scheme 4** as previously reported in literature.[51-52] This was accomplished by withdrawing aliquots from the reaction mixture at regular time intervals and subjecting the sample ESI-MS analyses. From the data obtained, the ATH mechanism is proposed to begin with the homolytic cleavage of the dinuclear complex **Ni4** in iPrOH to give the mononuclear species (**4a**) as detected from mass spectrum (m/z = 559.06 amu). This structural rearrangement may explain the relatively longer induction profiles observed in the kinetic plots (**Fig. S28**) and absence of molecular mass of the dinuclear complex **Ni4** in the spectrum (**Fig. S28**). The formation of the mononuclear aqua **Ni3a** complex also supports this transformation. Coordination of iPrOK to **4a** via substitution of the bromides to afford the Ni(**L4**)$_2$-(iPrO)$_2$ adduct (**4b**) was deduced from the m/z signal at 599 amu. Generation of the dihydride intermediate (**4c**), believed to be the active species followed by elimination of the acetone molecule could be hypothesized from the presence of the signal at m/z = 481 amu. Subsequent coordination of acetophenone substrate to form adduct (**4d**) prior to hydride migration to give the expected 1-phenyl ethanol product is evident from the signal at m/z = 657.14 amu corresponding to (**4e**). Elimination of the product from the metal coordination sphere is believed to complete the catalytic cycles leading to re-generation of the solvated complex (**4b**).
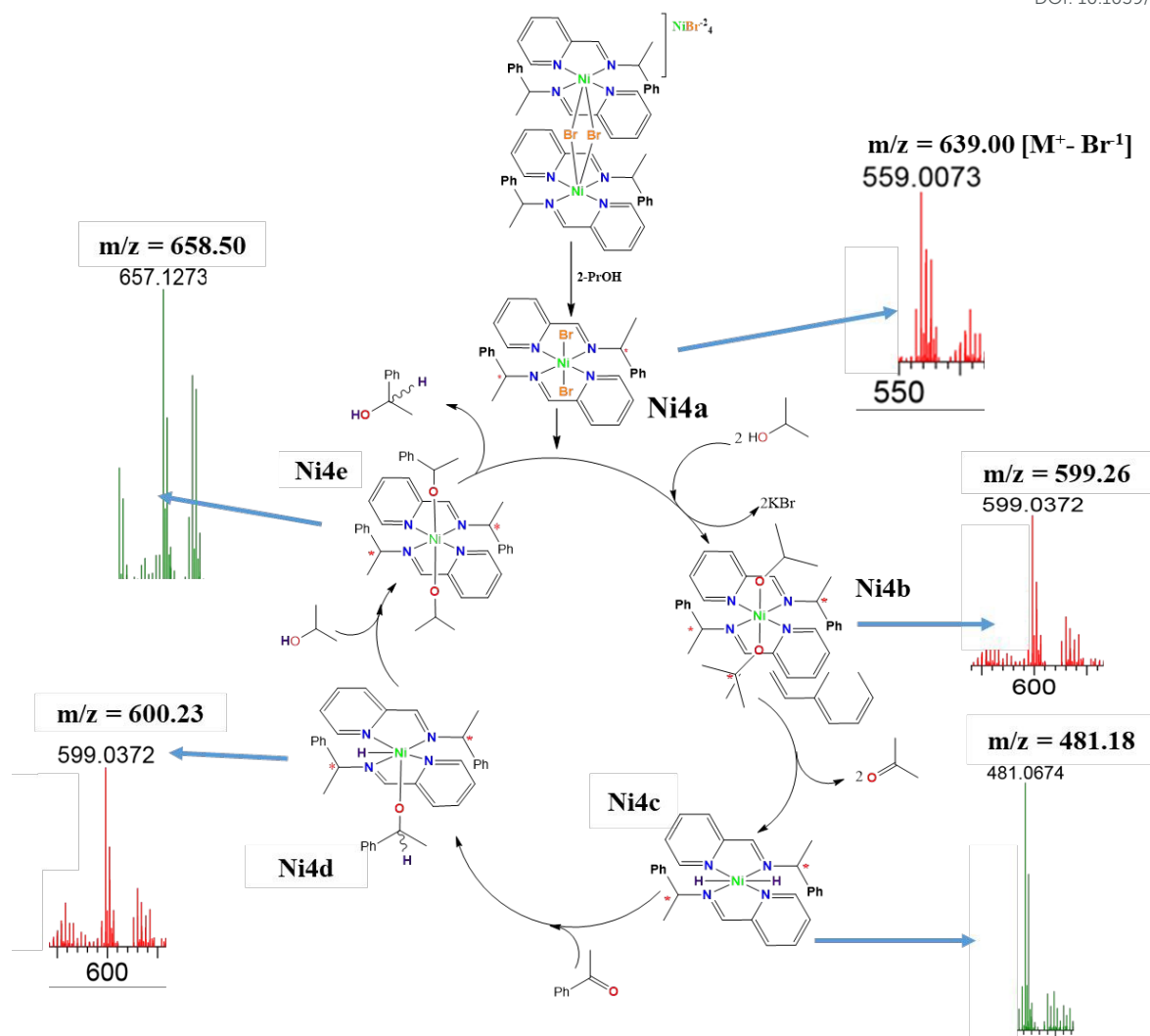
Scheme 4. Proposed mechanism of asymmetric transfer hydrogenation of ketones catalyzed by complex **Ni4** based on intermediates as identified from low resolution mass spectrometry.

Conclusions

In summary, chiral (pyridyl)imine Ni(II) complexes have been synthesized and structurally characterized using IR spectroscopy, mass spectrometry, single crystal X-ray crystallography and electron paramagnetic resonance. The complexes demonstrate some unprecedented diverse coordination chemistry controlled largely by the lability of the coordinated halides. The presence of two ligand units per Ni(II) atom in the dinuclear core

is unusual and highlight the less steric demands of the ligands. All the complexes showed moderate catalytic activities in the asymmetric transfer hydrogenation of ketones though with low enantioselectivity. The catalytic activities of the complexes were influenced by the ligand motif and nature of the base employed. The reactivities of the ketone substrates are controlled by both steric parameters and electronic factors. Kinetics data, sub-stoichiometric and mercury poisoning tests point to the homogeneity of the complexes with the formation of Ni(0) nanocluster particles. From low resolution mass spectrometry analyses of the reaction intermediates, a dihydride mechanism can be proposed.

3. Experimental sections

3.1 Materials and instrumentation

All synthetic manipulations especially reactions involving air and moisture sensitive materials were performed under nitrogen atmosphere using standard Schlenk techniques in a vacuum line. All solvents were of analytical grade. Toluene, hexane, dichloromethane (CH_2Cl_2), isopropanol (iPrOH), diethyl ether, ethyl acetate and ethanol were purified by distillation and dried over sodium/ benzophenone, $CaCl_2$ and molecular sieves prior to use. Starting materials: Nickel(II) bromide ethylene glycol dimethyl ether [$NiBr_2(DME)$] ($\geq$: 99.99%); Nickel Chloride ($NiCl_2$) ($\geq$ 99.99%), The ligands (*S*-)-1-phenyl-N-(pyridine-2-yl) ethylidene) ethanamine (**L1**), (*R*-)-1-phenyl-*N*-(pyridine-2-yl) ethylidine) ethanamine (**L2),** (S)-1-phenyl-N-(pyridine-2-yl methylene) ethanamine (**L3**) and (R)-1-phenyl-N-(pyridine-2yl methylene) ethanamine (**L4**) were synthesised by following literature procedure.[53] 2acetylpyridine ($\geq$ 99.99%), ($\geq$ 99.9%)2-propanol (iPrOH), acetophenone ($\geq$99.99%), KOH, NaOH, potassium tert-butoxide, Na_2CO_3, 2-chloro-acetophenol ($\geq$ 99.99%), 2-methyl acetophenone ($\geq$ 99.99%), 2-hydroxyacetophenone ($\geq$ 99.99%), 2-acetyl pyridine ($\geq$99.99%), acetyl pyrizine ($\geq$99.99%), 1-cyclohexyl-2-enyl) ethanone ($\geq$99.99%), cyclohexyl(phenyl)

methanone (≥99.99%), 1-naphthalen-3-yl) ethanone, (2- and aminophenyl) methanone, and (*R*) and (*S*-) 1-phenyl ethanol (≥ 99.99%), tricyclohexylphosphine (≥99.99%), triphenylphosphine (PPh$_3$) (≥ 99.99%), mercury (Hg), and Carbon disulfide (CS$_2$) (≥ 99.99%) were purchased from Sigma-Aldrich., and NMR solvents (deuterated chloroform, CDCl$_3$) were purchased from Sigma-Aldrich and used as received without further purification.

^{1}H and ^{13}C NMR spectra were recorded on a Bruker Ultrashield 400 (^{1}H NMR 400MHz, ^{13}C NMR 100 MHz) spectrometer in CDCl$_3$ solution at room temperature and chemical shifts (δ) were determined relative to internal TMS and recorded in ppm relative to CHCl$_3$ δ^1_H: 7.26 ppm and δ^{13}C: 77.6 ppm and DMSO-d$_6$ δ^1H; 2.50 ppm. Coupling constants (*J*) are reported in Hertz (Hz) and splitting patterns are indicated as s (singlet), d (doublet), dd (doublet of doublet), t (triplet), and m (multiplet). Elemental analyses were performed on Thermal Scientific Flash 2000, and ESI mass spectra were recorded on an LC premier micro-mass spectrometer. The infra-red spectra were recorded on a PerkinElmer spectrum 100 in the 4000 – 650 cm^{-1} range. EPR measurements were performed in the optical ERP cavity (ER 41040R, Bruker, Germany) employing a customly designed flat EPR cell equipped with a laminated Pt-mesh working electrode, Pt-wire as a counter electrode, and Agwire as a pseudo-reference electrode. The measurements were performed at X-band using a Bruker EPR spectrometer. The asymmetric transfer hydrogenation reaction of ketone was carried out in a two-necked round bottom flask fitted with a reflux condenser under nitrogen gas. GC analyses for enantiomeric excess were performed under the following chromatography conditions: Varian CP-3800, ga 265/ 51nm/ pst2, 5µl capillary 30m x 0.250 x 0.25 µm. Nitrogen carrier column gas 5psi, injector temperature 250 ^{o}C, oven programmed at isotherm 120 ^{O}C, 150:1 split ratio, flow rate = 1.5, velocity = 38cm/sec, 1*u*L sample and mobile phase (N$_2$) gas, internal standard: decane.

3.2. Synthesis and characterization of Ni(II) complexes

3.2.1. [Ni$_2$(L1)$_4$-µ-Br$_2$] [NiBr$_4$] (Ni1)

To a solution of [NiBr$_2$(DME)] (0.20 g, 0.65 mmol) in CH$_2$Cl$_2$ (15 mL), was added to solution of ligand (**L1**) (0.30 g, 1.30 mmol) in CH$_2$Cl$_2$ (15 mL) and the reaction was stirred at room temperature for 24 h to give a pink solution. After the specified reaction period, the resulting solution was concentrated under reduced pressure followed by addition hexane (20 ml) to precipitate crude product. The crude product was washed then with hexane (15 mL) and dried under vacuum to afford complex **1** as a green powder. Yield = 0.41 g, (50%). ESI-MS: m/z (%) 587 [1/2M − Br, 45%]$^+$, 362 [1/2M − (**L1**+Br), 100%]$^+$. FT-IR (cm^{-1}): (ν$_{C=N}$)$_{imine}$ =1649, µ$_{eff}$ = 3.97 BM. Anal. Calc. for C$_{60}$H$_{64}$N$_8$Ni$_3$Br$_6$: C, 46.28; H, 4.15; N, 7.22 Found: C, 46.29; H, 4.18; N, 7.26.

Complexes **Ni2- Ni5** were synthesised following the protocol described for **Ni1.**

3.2.2. Ni$_2$(L2)$_4$-µ-Br$_2$] [NiBr$_4$] (Ni2)

[NiBr$_2$(DME)] (0.20 g, 0.65 mmol) in CH$_2$Cl$_2$ (15 mL) and **L2** (0.30 g, 1.30 mmol) in CH$_2$Cl$_2$ (15 mL) to afford green powder. Yield = 0.48 g (58%). ESI-MS: *m/z* (%) 587 [1/2M − Br, 100%]$^+$, 362 [1/2M − (**L1**+Br), 60%]$^+$. FT-IR (cm^{-1}): (ν$_{C=N}$)$_{imine}$ = 1639, µ$_{eff}$ = 3.76 BM. Anal. Calc. for C$_{60}$H$_{64}$N$_8$Ni$_3$Br$_6$. C, 46.41; H, 4.15; N, 7.22 Found: C, 46.46; H, 4.20; N, 7.24.

3.2.2. [Ni$_2$(L3)$_4$-µ-Br$_2$] [Br$_2$] (Ni3)

[NiBr$_2$(DME)] (0.10 g, 0.33 mmol) in CH$_2$Cl$_2$ (15 mL) and **L3** (0.14 g, 0.65 mmol) in CH$_2$Cl$_2$ (15 mL) to afford lemon green powder. Yield = 0.43g (52%). ESI-MS: *m/z* (%) 559 [1/2M − Br, 100%]$^+$, FT-IR (cm^{-1}): (ν$_{C=N}$)$_{imine}$ = 1650, (ν$_{C=N}$)$_{py}$ = 3291. EPR (CH$_2$Cl$_2$, liquid N$_2$

temperature): g = 2.2836. μ_{eff} = 3.52 BM. Recrystallization from a mixture of CH_2Cl_2: hexane

solution afforded single crystals suitable for single crystal X-ray crystallography.

$C_{56}H_{56}N_8Ni_2Br_4$: C, 52.62; H, 4.42; N, 8.77. Found: C, 52.60; H, 4.49; N, 8.81.

3.2.4. [Ni₂(*L4*)₄-µ-Br₂] [NiBr₄] (*Ni4*)

[$NiBr_2(DME)$] (0.20 g, 0.65 mmol) in CH_2Cl_2 (10 mL) and **L4** (0.28 g, 1.30 mmol) in

CH_2Cl_2 (10 mL) to afford lemon green powder. Yield = 0.51g (56 %). ESI-MS: *m/z* (%) 559

[1/2M – Br, 100%]$^+$. FT-IR (cm^{-1}): $(v_{C=N})_{imine}$ = 1641, $(v_{C=N})_{py}$ = 3388. EPR (CH_2Cl_2, liquid

N_2 temperature): g = 2.28. μ_{eff} = 3.66 BM. Recrystallization from a mixture of CH_2Cl_2: hexane

solution afforded single crystals suitable for single crystal x-ray crystallography. Anal. Calc.

for Anal. Calc. for $C_{56}H_{56}N_8Ni_3Br_6$: C, 44.94; H, 3.77; N, 7.49. Found: C, 44.81; H, 3.91; N,

7.65.

3.2.5. [Ni(L3)₂Cl₂] (*Ni5*)

NiCl2 (0.20 g, 1.5 mmol) in CH_2Cl_2 (10 mL) and **L4** (0.63 g, 3.00 mmol) in CH_2Cl_2 (10 mL)

to afford a lemon green powder. Yield = 0.51g (58 %). ESI-MS: *m/z* (%) 483 [M –2Cl, 100%]$^+$.

FT-IR (cm^{-1}): $(v_{C=N})_{imine}$ = 1631, EPR (CH_3N, liquid N_2 temperature): g = 2.2. μ_{eff} = 3.62 BM.

Recrystallization from a mixture of CH_3CN: $(CH_3CH_3)_2O$ solution afforded single crystals

suitable for single crystal x-ray crystallography. Anal. Calc. for Anal. Calc. for

$C_{28}H_{28}N_4NiCl_2$: C, 61.13; H, 5.13; N, 10.18. Found: C, 61.14; H, 5.21; N, 10.15.

3.3. Single crystal X-ray crystallography

Single crystal X-ray diffraction data collection and structure refinement for **Ni3, Ni4** and **Ni5**

were recorded on a Bruker Apex Duo equipped with an Oxford Instrument Cryo jet operating

at 100(2) K and an uncoated micro source operating at 30 W power. The data were collected

Dalton Transactions

with Mo Kα (λ = 0.71073 (Å)) radiation at a crystal-to-detector distance of 50 mm. The following conditions were used for the data collection: omega and phi scans with exposures taken at 30 W X-ray power and 0.50 frame widths using APEX2.[54] The data were reduced with the programme SAINT[55] using outlier rejection, scan speed scaling, as well as standard Lorentz and polarisation correction factors. A SADABS semi-empirical multi-scan absorption correction was applied to the data. Direct methods, SHELXS-2014 and WinGX were used to solve both structures. All non-hydrogen atoms were located in the difference density map and refined anisotropically with SHELX-2014.[56] All hydrogen atoms were included as idealized contributors in the least squares process. Their positions were calculated using a standard riding model with C-H$_{aromatic}$ distances of 0.93 Å and U$_{iso}$ = 1.2Ueq and CH$_{methylene}$ distances of o.99 Å and U$_{iso}$ =1.2 U_{eq} and C-H$_{methyl}$ distances of 0.98 Å and U$_{iso}$ =1.5 U_{eq}.

3.4. General procedure for asymmetric transfer hydrogenation of ketones

For catalytic asymmetric transfer hydrogenation of ketones, a typical procedure was as followed. A solution of 5 mL of KOH (100 mmol %) in iPrOH and catalysts **Ni1-Ni5** (0.3.0 mmol %) were mixed and stirred at 82 °C for 30 min, 2.0 mmol of ketone was introduced in drop wise into the reaction mixture. During the process of reaction, about 0.5 mL of the mixture was sampled at regular time intervals, cooled, and percentage conversion of acetophenone to 1-phenyl ethanol was analysed using ^{1}H NMR spectroscopy by comparing the intensity of methyl signals of acetophenone (s, δ 2.59 ppm) and 1-phenyl ethanol (d, δ 1.49 ppm) of the crude products. In addition, GC was used as a standard to validate the results and also to determine the enantiomeric excess (*ee* %). Kinetic data were analysed using 64-bit Origin Pro 9.1. A standard nonlinear first order monomolecular exponential growth model, $y = e^{a(1 - e(k(x-xc)))}$, where a = amplitude, x = time, x$_c$ = centre, and k = rate, was used to fit the kinetic data for **Ni1–Ni5**.

3.5. Mercury poisoning tests

In a typical experiment, to a solution of the pre-activated catalyst system (complex **Ni4,** 0.3% mmol, in 5 mL of KOH,100 mmol%; in iPrOH 5 mL), acetophenone (2.0 mmol) and the respective amounts of Hg (3, 5 and 10 drops) were added and allowed to reflux at 82 ℃ for 24 h. During the reaction, about 0.5 mL of the reacting mixture was sampled at regular time intervals, cooled and analysed for percentage conversion. In the second test, 3 drops of Hg were added at 50% conversion (time, t = 4.5 h and 8 h respectively) and allowed to proceed for 24 h during which samples were withdrawn at regular time intervals and analysed for percentage conversion.

3.6. Sub-stoichiometric deactivation studies

To a solution of pre-activated catalyst system (complex **Ni4,** 0.3% mmol, in 5 mL of KOH,100 mmol%; in iPrOH 5 mL), acetophenone (2.0 mmol) and 20% mol equivalent of the appropriate poisoning agent, carbon disulphide (CS_2), triphenylphosphine (PPh_3), and tricyclohexyl phosphine ($PCy)_3$ was added and allowed to reflux at 82 ℃ for 24 h. During thi period, samples were withdrawn at regular time intervals, cooled and analysed as discussed in section 3.4.

3.7. Mechanistic studies of ATH of ketones

Mechanistic studies of the transfer hydrogenation of acetophenone catalyzed by nickel complexes were performed using low resolution ESI-MS technique. Generally, a solution of the nickel complex (0.3 mol% **Ni1**-**Ni5**) in iPrOH were mixed and stirred at 82 ℃ for 30 min followed by drop-wise addition of acetophenone (2.0 mmol) in iPrOH (5 mL) into the reaction mixture and stirred for 24 h. During the course the reaction, about 0.1 mL of the mixture was sampled at regular time intervals, cooled to about 0 ℃ and analysed using ESI-MS technique to identify the respective mass fragments of the intermediates in the catalytic cycle.

References

1.	Chen, J.-s.; Li, Y.-y.; Dong, Z.-r.; Li, B.-z.; Gao, J.-x., *Tetrahedron Let.***2004,** *45*, 8415-8418.

2.	Wan, K. Y.; Roelfes, F.; Lough, A. J.; Hahn, F. E.; Morris, R. H., *Organometallics* **2018,** *37*, 491-504.

3.	Goldberg, K.; Schroer, K.; Lütz, S.; Liese, A., *Appl. Microbio.biotech.* **2007,** *76*, 237.

4.	Hashiguchi, S.; Fujii, A.; Takehara, J.; Ikariya, T.; Noyori, R., *J. Am. Chem. Soc.* **1995,** *117*, 7562-7563.

5.	Gao, J.-X.; Ikariya, T.; Noyori, R., *Organometallics* **1996,** *15* 1087-1089.

6.	Faller, J.; Lavoie, A. R., *Organometallics* **2002,** *21*, 3493-3495.

7.	Bertoli, M.; Choualeb, A.; Lough, A. J.; Moore, B.; Spasyuk, D.; Gusev, D. G., *Organometallics* **2011,** *30*, 3479-3482.

8.	Wang, D.; Astruc, D., *Chem. Rev.* **2015,** *115*, 6621-6686.

9.	Clarke, Z. E.; Maragh, P. T.; Dasgupta, T. P.; Gusev, D. G.; Lough, A. J.; Abdur-Rashid, K., *Organometallics* **2006,** *25*, 4113-4117.

10.	Werkmeister, S.; Neumann, J.; Junge, K.; Beller, M., *Chem. Eur. J.* **2015,** *21*, 12226-12250.

11.	Baratta, W.; Ballico, M.; Del Zotto, A.; Siega, K.; Magnolia, S.; Rigo, P., *Chem. Eur. J.* **2008,** *14*, 2557-2563.

12.	Wu, X.; Li, X.; Zanotti-Gerosa, A.; Pettman, A.; Liu, J.; Mills, A. J.; Xiao, J., *Chem. Eur. J.* **2008,** *14*, 2209-2222.

13.	Morris, R. H., *Chem. Soc. Rev.***2009,** *38*, 2282-2291.

14.	Demmans, K.; Ko, O.; Morris, R., *RSC Adv.* **2016,** *6*, 88580-88587.

15.	Malacea, R.; Poli, R.; Manoury, E., *Coord. Chem. Rev.* **2010,** *254*, 729-752.

16.	Wu, X.; Xiao, J., *Chem. Commun.* **2007,** , 2449-2466.

Dalton Transactions Accepted Manuscript

17.   Abubakar, S.; Bala, M. D., *J. Coord. Chem.* **2018,** *71*, 2913-2923.

18.   Foubelo, F.; Najera, C.; Yus, M., *Tetrahedron: Asymmetry* **2015,** *26*, 769-790.

19.   Dong, Z. R.; Li, Y. Y.; Yu, S. L.; Sun, G. S.; Gao, J. X., *Chin. Chem. Let.* **2012,** *23*, 533-536.

20.   Magubane, M. N.; Nyamato, G. S.; Ojwach, S. O.; Munro, O. Q., *RSC Adv.* **2016,** *6*, 65205-65221.

21.   Magubane, M. N.; Alam, M. G.; Ojwach, S. O.; Munro, O. Q., *J. Mol. Struc.* **2017,** *1135*, 197-201.

22.   Cotton, F. A.; Wilkinson, G.; Murillo, C. A.; Bochmann, M.; Grimes, R., *Adv. Inorg. Chem.* Wiley New York: 1988; Vol. 6.

23.   Atkins, P.; Overton, T., *Shriver and Atkins' Inorg. Chem..* Oxford University Press, USA: 2010.

24.   Riggle, K.; Lynde-Kernell, T.; Schlemper, E., *J. Coord. Chem.* **1992,** *25*, 117-125.

25.   Liu, X.; Zhang, J.; Yang, L.; Hase, W. L., *J. Am. Chem. Soc.* **2018,** *140*, 10995-11005.

26.   Bruno, I. J.; Cole, J. C.; Edgington, P. R.; Kessler, M.; Macrae, C. F.; McCabe, P.; Pearson, J.; Taylor, R., *Acta Crystallog. Sec. B: Struc. Sci.* **2002,** *58*, 389-397.

27.   Allen, F. H., *Acta Crystallog. Sec. B: Struc. Sci.* **2002,** *58*, 380-388.

28.   Cazacu, M.; Shova, S.; Soroceanu, A.; Machata, P.; Bucinsky, L.; Breza, M.; Rapta, P.; Telser, J.; Krzystek, J.; Arion, V. B., *Inorg. Chem.* **2015,** *54*, 5691-5706.

29.   Mohanan, K.; Murukan, B., *Synth. Reac. Inorg., Met. Org., Nano-Met. Chem.* **2005,** *35*, 837-844.

30.   Atkins, P. W.; De Paula, J.; Keeler, J., *Atkins' Phys. Chem.* 11th ed.; Oxford University Press: Oxford, 2018.

31.   Tondreau, A. M.; Lobkovsky, E.; Chirik, P. J., *Org. Let.* **2008,** *10*, 2789-2792.

32. Castellanos-Blanco, N.; Arévalo, A.; García, J. J., *Dalton Transac.* **2016,** *45,* 13604-13614.

33. Bartholomew, C. H., *Appl. Catal. Gen.* **2001,** *212*, 17-60.

34. van Leeuwen, P. W., *Applied Catalysis A: General* **2001,** *212*, 61-81.

35. Prabhu, R. N.; Ramesh, R., *J. Organomet. Chem.* **2012,** *718*, 43-51.

36. Aupoix, A.; Bournaud, C.; Vo-Thanh, G., *Eur. J. Org. Chem.* **2011,** *2011*, 2772-2776.

37. Bigler, R.; Mezzetti, A., *Org. Proc. Res. & Dev.* **2016,** *20*, 253-261.

38. Bigler, R.; Huber, R.; Stöckli, M.; Mezzetti, A., *ACS Catal.* **2016,** *6*, 6455-6464.

39. Liu, T.; Chai, H.; Wang, L.; Yu, Z., *Organometallics* **2017,** *36* , 2914-2921.

40. Aiken III, J. D.; Finke, R. G., *J. Mol. Catal. A: Chem.* **1999,** *145*, 1-44.

41. Sonnenberg, J. F.; Morris, R. H., *Catal. Sci. & Tech.* **2014,** *4*, 3426-3438.

42. Sonnenberg, J. F.; Morris, R. H., *ACS Catal.* **2013,** *3*, 1092-1102.

43. Bayram, E.; Linehan, J. C.; Fulton, J. L.; Roberts, J. A.; Szymczak, N. K.; Smurthwaite, T. D.; Ozkar, S.; Balasubramanian, M.; Finke, R. G., *J. Am. Chem. Soc.* **2011,** *133*, 18889-18902.

44. Schmidt, A.; Kurokhtina, A., *Kinet. and Catal.***2012,** *53*, 714-730.

45. Hornstein, B. J.; Aiken, J. D.; Finke, R. G., N, *Inorg. chem.* **2002,** *41*, 1625-1638.

46. Watzky, M. A.; Finke, R. G., *J. Am. Chem. Soc.* **1997,** *119*, 10382-10400.

47. Alley, W. M.; Hamdemir, I. K.; Wang, Q.; Frenkel, A. I.; Li, L.; Yang, J. C.; Menard, L. D.; Nuzzo, R. G.; Ozkar, S.; Yih, K.-H., *Langmuir* **2011,** *27*, 6279-6294.

48. Jaska, C. A.; Temple, K.; Lough, A. J.; Manners, I., *J. Am. Chem. Soci.* **2003,** *125*, 9424-9434.

49. Hagen, C. M.; Widegren, J. A.; Maitlis, P. M.; Finke, R. G., *J. Am. Chem. Soc.* **2005,** *127*, 4423-4432.

50.   Touge, T.; Nara, H.; Fujiwhara, M.; Kayaki, Y.; Ikariya, T., *J. Am. Chem. Soc.* **2016,** *138*, 10084-10087.

51.   Vikse, K. L.; Ahmadi, Z.; McIndoe, J. S., *Coord. Chem. Rev.* **2014,** *279*, 96-114.

52.   Müller, C. A.; Markert, C.; Teichert, A. M.; Pfaltz, A., *Chem. Commun.* **2009,** 1607-1618.

53.   Nayab, S.; Lee, H.; Jeong, J. H., *Polyhedron* **2012,** *43*, 55-62.

54.   APeX, B., SAINT and SADABS. *Bruker AXS., Madison, Wisconsin, USA* **2010**.

55.   Sheldrick, G. M.,. *Acta Crystallog. Sec. A: Found. Crystallog.* **2008,** *64*, 112-122.

56.   Farrugia, L. J., *J. Appl. Crystallog.* **2012,** *45*, 849-854.